

Color Spaces and Digital Imaging

Higham, Nicholas J.

2015

MIMS EPrint: **2015.85**

Manchester Institute for Mathematical Sciences
School of Mathematics

The University of Manchester

Reports available from: <http://eprints.maths.manchester.ac.uk/>

And by contacting: The MIMS Secretary
School of Mathematics
The University of Manchester
Manchester, M13 9PL, UK

ISSN 1749-9097

Color Spaces and Digital Imaging[†]

Nicholas J. Higham

1 Vector Space Model of Color

The human retina contains photoreceptors called cones and rods that act as sensors for the human imaging system. The cones come in three types, with responses that peak at wavelengths corresponding to red, green, and blue light, respectively; see figure 1. Rods are of a single type and produce only monochromatic vision; they are used mainly for night vision. Because there are three types of cones, color theory is replete with terms having the prefix “tri”. In particular, *trichromacy*, developed by Young, Grassmann, Maxwell, and Helmholtz, is the theory that shows how to match any color with an appropriate mixture of just three suitably chosen primary colors.

We can model the responses of the three types of cones to light by the integrals

$$c_i(f) = \int_{\lambda_{\min}}^{\lambda_{\max}} s_i(\lambda) f(\lambda) d\lambda, \quad i = 1: 3, \quad (1)$$

where f describes the spectral distribution of the light hitting the retina, s_i describes the sensitivity of the i th cone to different wavelengths, and $[\lambda_{\min}, \lambda_{\max}] \approx [400 \text{ nm}, 700 \text{ nm}]$ is the interval of wavelengths of the visible spectrum. Note that this model is linear ($c_i(f + g) = c_i(f) + c_i(g)$) and it projects the spectrum onto the space spanned by the $s_i(\lambda)$ —the “human visual subspace.”

For computational purposes a grid of n equally spaced points λ_i on the interval $[\lambda_{\min}, \lambda_{\max}]$ is introduced and the repeated rectangle (or midpoint) quadrature rule is applied to (1), yielding

$$c = S^T f, \quad c \in \mathbb{R}^3, \quad S \in \mathbb{R}^{n \times 3}, \quad f \in \mathbb{R}^n,$$

where the i th column of the matrix S has samples of s_i at the grid points, the vector f contains the values of $f(\lambda)$ at the grid points, and the vector c absorbs constants from the numerical integration. In practice, a value of n around 40 is typically used.

Let the columns of $P = [p_1 \ p_2 \ p_3] \in \mathbb{R}^{n \times 3}$ represent *color primaries*, defined by the property that the 3×3 matrix $S^T P$ is nonsingular. For example,

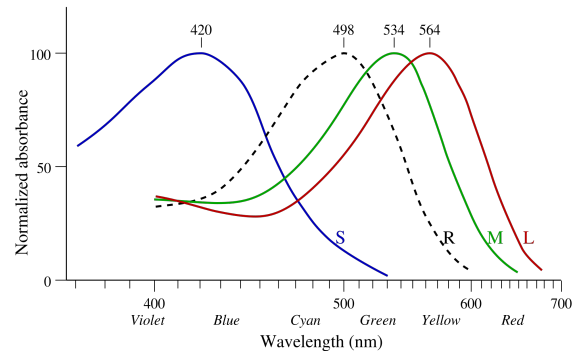


Figure 1 Response curves for the cones and the rods (dotted line). S, M, and L denote the cones most sensitive to short (blue), medium (green) and long (red) wavelengths, respectively. Figure from (Wikimedia Commons)

<http://en.wikipedia.org/wiki/File:Cone-response.svg>

p_1 , p_2 , and p_3 could represent red, blue, and green, respectively. We can write

$$S^T f = S^T P (S^T P)^{-1} S^T f \equiv S^T P a(f), \quad (2)$$

where $a(f) = (S^T P)^{-1} S^T f \in \mathbb{R}^3$. This equation shows that the color of any spectrum f (or more precisely the response of the cones to that spectrum) can be matched by a linear combination, $P a(f)$, of the primaries. A complication is that we need all the components of a to be nonnegative for this argument, as negative intensities of primaries cannot be produced. A way around this problem is to write $a(f) = a_1 - a_2$, where a_1 contains the nonnegative components of $a(f)$ and a_2 has positive components, and rewrite (2) as

$$S^T (f + P a_2) = S^T P a_1.$$

This equation says that $P a_1$ matches f with appropriate amounts of some of the primaries added. This rearrangement is a standard trick in *colorimetry*, which is the science of color measurement and description.

To summarize, the color of a visible spectrum f can be matched by *tristimulus values* $a(f) = A^T f$, where $A^T = (S^T P)^{-1} S^T$, because $S^T f = S^T P a(f)$. The columns of $A \in \mathbb{R}^{3 \times n}$ are called (samples of) color matching functions for the given primaries.

To determine A a human observer is asked to match light of single wavelengths λ_i by twiddling knobs to mix light sources comprising the three primaries until a match is obtained. Light of a single wavelength corresponds to a vector $f = e_i$, where e_i has a 1 in the i th position and zeros everywhere else, and the vector $a(f) = A^T f$ that gives the match is therefore the

[†]. Author’s final version, before copy editing and cross-referencing, of: N. J. Higham. Color spaces and digital imaging. In N. J. Higham, M. R. Dennis, P. Glendinning, P. A. Martin, F. Santosa, and J. Tanner, editors, *The Princeton Companion to Applied Mathematics*, pages 808–813. Princeton University Press, Princeton, NJ, USA, 2015.

i th column of A^T . In this way we can determine the color matching matrix A corresponding to the given primaries.

This vector space model of color is powerful. For example, since the $3 \times n$ matrix S^T has a nontrivial null space it tells us that there exist spectra f and g with $f \neq g$ such that $S^T f = S^T g$. Hence two colors can look the same to a human observer but have a different spectral decomposition, which is the phenomenon of *metamerism*. This is a good thing in the sense that color output systems (such as computer monitors) exploit metamerism to reproduce color. There is another form of metamerism that is not so welcome: when two colors appear to match under one light source but do not match under a different light source. An example is when you put on socks in the bedroom with the room lights on and they appear black, but when you view them in daylight one sock turns out to be blue.

The use of linear algebra in understanding color was taken further by Jozef Cohen (1921-1995), whose work is summarized in the posthumous book *Visual Color and Color Mixture: The Fundamental Color Space* (2001). Cohen stresses the importance of what he calls the “matrix R ”, defined by

$$R = S(S^T S)^{-1} S^T = S S^+,$$

where S^+ is the Moore-Penrose pseudoinverse of S . Mathematically, R is the orthogonal projector onto $\text{range}(S)$. Cohen noted that R is independent of the choice of primaries used for color matching, that is, R is unchanged under transformations $S \leftarrow SZ$ for nonsingular $Z \in \mathbb{R}^{3 \times 3}$, and so is an invariant. He also showed how in the factorization $S = QL$, where $Q \in \mathbb{R}^{n \times 3}$ has orthonormal columns and $L \in \mathbb{R}^{3 \times 3}$ is lower triangular, the factor Q (which he called F) plays an important role in color theory through the use of “tricolor coordinates” $Q^T f$.

We do not all see color in the same way: about 8% of males and 0.5% of females are affected by color blindness. The first investigation into color vision deficiencies was by Manchester chemist John Dalton (1766-1844), who described his own color blindness in a lecture to the Manchester Literary and Philosophical Society. He thought that his vitreous humor was tinted blue and instructed that his eyes be dissected after his death. No blue coloring was found but his eyes were preserved. A DNA analysis in 1985 concluded that Dalton was a deuteranope, meaning that he lacked cones sensitive to the medium wavelengths (green). The color

model and analogues of figure 1 for different cone deficiencies help us to understand color blindness.

Given the emphasis in this section on trichromacy, one might wonder why printing is usually done with a four color CMYK model when three colors should be enough. CMYK stands for cyan-magenta-yellow-black, and cyan, magenta, and yellow are complementary colors to red, green, and blue, respectively. Trichromatic theory says that a CMY system is entirely adequate for color matching, so the K component is redundant. The reason for using K is pragmatic. Producing black in a printing process by overlaying C, M, and Y color plates uses a lot of ink, makes the paper very wet, and does not produce a true, deep black due to imperfections in the inks. In CMYK printing *gray component replacement* is used to replace proportions of the CMY components that produce gray with corresponding amounts of K. (A naive algorithm to convert from CMY to CMYK is $K = \min(C, M, Y)$, $C \leftarrow C - K$, $M \leftarrow M - K$, $Y \leftarrow Y - K$, though in practice slightly different amounts of C, M, and Y are required to produce black.)

2 Standardization

The Commission Internationale de l’Éclairage (CIE) is responsible for standardization of color metrics and terminology. Figure 2 shows the standard RGB color matching functions produced by the CIE (1931, 1964). They are based on color matching experiments and correspond to primaries at 700 nm (red), 546.1 nm (green), and 435.8 nm (blue). The red curve takes negative values as shown in the figure, but nonnegative functions were preferred for calculations in the pre-computer era as they avoided the need for subtractions. So a CIE XYZ space was defined that has nonnegative color matching functions (see figure 3), and which is obtained via the linear mapping¹

$$\begin{bmatrix} X \\ Y \\ Z \end{bmatrix} = \begin{bmatrix} 0.49 & 0.31 & 0.20 \\ 0.17697 & 0.81240 & 0.01063 \\ 0 & 0.01 & 0.99 \end{bmatrix} \begin{bmatrix} R \\ G \\ B \end{bmatrix}.$$

Two of the choices made by the CIE that led to this transformation are that the Y component approximates the perceived brightness, called the *luminance*, and that $R = G = B = 1$ corresponds to $X = Y = Z = 1$, which requires that the rows of the matrix sum to 1.

Because the XYZ space is three-dimensional it is not easy to visualize the subset of it corresponding to

1. The coefficients of the matrix are written here in a way that indicates their known precision. Thus, for example, the (1,1) element is known to two significant digits but the (2,1) element is known to five significant digits.

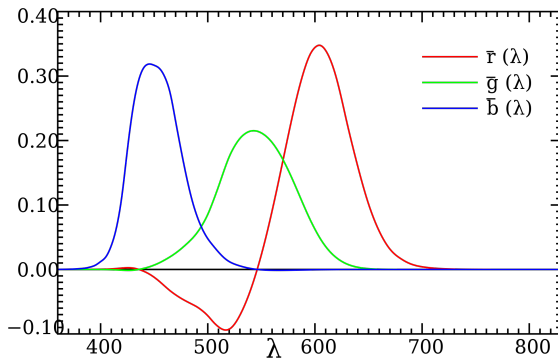


Figure 2 CIE RGB color matching functions from the 1931 standard. Figure from (Wikimedia Commons) http://en.wikipedia.org/wiki/File:CIE1931_RGBCMF.svg

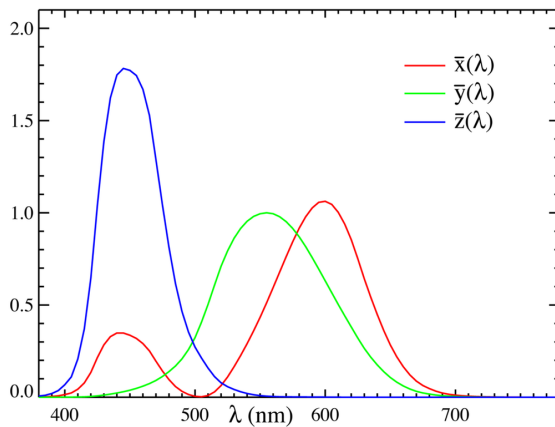


Figure 3 CIE XYZ color matching functions from the 1931 standard. Figure from (Wikimedia Commons) http://en.wikipedia.org/wiki/File:CIE1931_XYZCMF.png

the visible spectrum. It is common practice to use a projective transformation

$$x = \frac{X}{X+Y+Z}, \quad y = \frac{Y}{X+Y+Z} \quad (z = 1 - x - y)$$

to produce a *chromaticity diagram* in terms of the (x, y) coordinates; see figure 4. The visible spectrum forms a convex set in the shape of a horseshoe. The curved boundary of the horseshoe is generated by light of a single wavelength (pure color) as it varies across the visible spectrum, while at the bottom the “purple line” is generated by combinations of red and blue light. The diagram represents color and not luminance, which is why there is no brown (a dark yellow). White is at $(\frac{1}{3}, \frac{1}{3})$

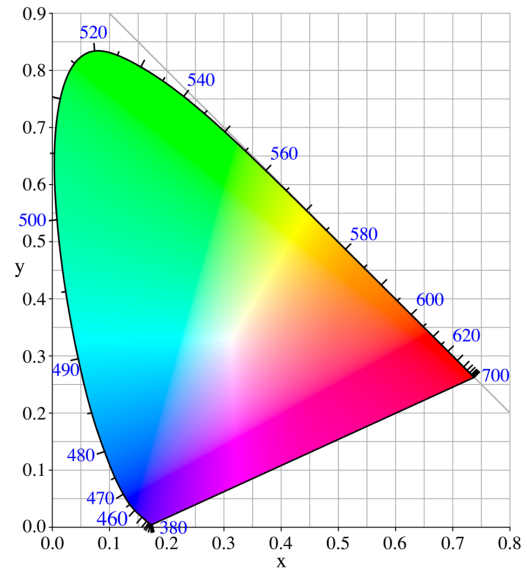


Figure 4 CIE 1931 color space chromaticity diagram, with the gamut of sRGB shown. Figure from (Wikimedia Commons) <http://en.wikipedia.org/wiki/File:CIExy1931.png>

and pure colors lying at opposite ends of a line passing through the white point are complementary: a combination of them produces white. Any point outside this region represents an “imaginary color”: a distribution of light that is not visible to us.

A common use of the chromaticity diagram is in reviews of cameras, scanners, displays, and printers, where the gamut of the device (the range of producible colors) is overlaid on the diagram. Generally the closer the gamut is to the visible spectrum the better, but since images are passed along a chain of devices starting with a camera or scanner a key question is how the gamuts of the devices compare and whether colors are faithfully translated from one device to another. Color management deals with these issues, through the use of International Color Consortium (ICC) profiles that describe the color attributes of each device by defining a mapping between the device space and the CIE XYZ reference space. Calibrating a device involves solving nonlinear equations, which is typically done by Newton’s method.

3 Nonlinearities

So far, basic linear algebra and a projective transformation have been all that we need to develop color theory, and one might hope that by using more sophisticated

techniques from matrix analysis one can go further. To some extent, this is possible; for example, the Binet–Cauchy theorem on determinants finds application in several problems in colorimetry. But nonlinearities cannot be avoided for long, because human eyes respond to light nonlinearly, in contrast to a digital camera’s sensor, which has a linear response. The relative difference in brightness that we see between a dark cellar and bright sunlight is far smaller than the relative difference in the respective number of photons reaching our eyes, and this needs to be incorporated into the model. One way of doing this is described in the next section.

4 LAB Space

A problem with the CIE XYZ and RGB spaces is that they are far from being perceptually uniform, which means that there is not a linear relation between distances in the tristimulus space and perceptual differences. This led the CIE to search for nonlinear transformations that give more uniform color spaces, and in 1976 they came up with two standardized systems, $L^*u^*v^*$ and $L^*a^*b^*$ (or LAB, pronounced “ell-A-B”). In the LAB space the L coordinate represents lightness, the A coordinate is on a green–magenta axis, and the B coordinate is on a blue–yellow axis. For a precise definition in terms of the XYZ space, if X_n , Y_n , and Z_n are the tristimuli of white then

$$\begin{aligned} L &= 116f(Y/Y_n) - 16, \\ A &= 500 [f(X/X_n) - f(Y/Y_n)], \\ B &= 200 [f(Y/Y_n) - f(Z/Z_n)], \end{aligned}$$

where

$$f(x) = \begin{cases} x^{1/3}, & x \geq 0.008856, \\ 7.787x + \frac{16}{116}, & x \leq 0.008856. \end{cases}$$

The cube root term tries to capture the nonlinear perceptual response of human vision to brightness. The two cases in the formula for f bring in a different formula for low tristimulus values, i.e., low light. The lightness coordinate L ranges from 0 to 100. The A and B coordinates are typically in the range -128 to 128 (though not explicitly constrained) and $A = B = 0$ denotes lack of color, i.e., a shade of gray from black ($L = 0$) to white ($L = 100$). In colorimetry, color differences are expressed as Euclidean distances between LAB coordinates and are denoted ΔE .

An interesting application of LAB space is to the construction of color maps, which are used to map

numbers to colors when plotting data. The most commonly used color map is the rainbow color map, which starts at dark blue and progresses through cyan, green, yellow, orange, and red, through colors of increasing wavelength. In recent years the rainbow color map has been heavily criticized for a number of reasons, which include

- it is not perceptually uniform, in that the colors appear to change at different rates in different regions (faster in the yellow, slower in the green),
- it is confusing, because people do not always remember the ordering of the colors, making interpretation of an image harder,
- it loses information when printed on a monochrome printer, since high and low values map to similar shades of gray.

These particular criticisms can be addressed by using a color map constructed in LAB space with colors having monotonically increasing L values and linearly spaced A and B values. Color maps based on such ideas have supplanted the once ubiquitous rainbow color map as the default in MATLAB and in some visualization software.

For image manipulation there are some obvious advantages to working in LAB space, as luminosity and color can easily be independently adjusted, which is not the case in RGB space. However, LAB space has some strange properties. For example, $(L, A, B) = (0, 128, -128)$ represents a brilliant magenta as black as a cellar! LAB space contains many such imaginary colors that cannot exist and are not representable in RGB. For many years LAB was regarded as a rather esoteric color space of use only for intermediate representations in color management and the like, though it is supported in high end software such as Adobe Photoshop and the MATLAB Image Processing Toolbox. However, in recent years this view has changed, as photographers and retouchers have realized that LAB space, when used correctly, is a very powerful tool for manipulating digital images. The book *Photoshop LAB Color* (2006) by Dan Margulis describes the relevant techniques, which include ways to reduce noise (blur the A and B channels), massively increase color contrast (stretch the A and B channels), and change the color of colorful objects in a scene while leaving the less colorful objects apparently unchanged (linear transformations of the A and B channels). As an example of the latter technique, figure 5 shows at the top an RGB image of



Figure 5 Top: original image. Bottom: image converted to LAB space and A channel negated $((L, A, B,) \leftarrow (L, -A, B))$.

a building at the University of Manchester. At the bottom is the result of converting the image to LAB, flipping the sign of the A channel, then converting back to RGB. The effect is to change the turquoise paint to pink without, apparently, significantly changing any other color in the image including the blue sky. In truth, all the colors have changed, but mostly by such a small amount that the changes are not visible, due to the colors having small A components in LAB coordinates.

5 JPEG

JPEG is a compression scheme for RGB images that can greatly reduce file size, though it is lossy (throws information away). The JPEG process first converts from RGB to the $Y C_b C_r$ color space, where Y represents luminance and C_b and C_r represent blue and red chrominances, respectively, using the linear transformation

$$\begin{bmatrix} Y \\ C_b \\ C_r \end{bmatrix} = \begin{bmatrix} 0.299 & 0.587 & 0.114 \\ -0.1687 & -0.3313 & 0.5 \\ 0.5 & -0.4187 & -0.0813 \end{bmatrix} \begin{bmatrix} R \\ G \\ B \end{bmatrix}.$$

The motivation for this transformation is that human vision has a poor response to spatial detail in colored areas of the same luminance, so the C_b and C_r components can take greater compression than the Y component. The image is then broken up into 8×8 blocks and for each block a two-dimensional discrete cosine transform is applied to each of the components, after which

the coefficients are rounded, more aggressively for the C_b and C_r components. Of course, it is crucial that the 3×3 matrix in the above transformation is nonsingular, as the transformation needs to be inverted in order to decode a JPEG file.

The later JPEG2000 standard replaces the discrete cosine transform with a wavelet transform and uses larger blocks. Despite the more sophisticated mathematics underlying it, JPEG2000 has not caught on as a general purpose image format, but it is appropriate in special applications such as storing fingerprints, where it is much better than JPEG at reproducing edges.

6 Nonlinear RGB

The CIE LAB and XYZ color spaces are device-independent: they are absolute color spaces defined with reference to a “standard human observer.” The RGB images one comes across in practice, such as JPEG images from a digital camera, are in device-*dependent* RGB spaces. These spaces are obtained from a linear transformation of CIE XYZ space followed by a nonlinear transformation of each coordinate that modifies the gamma (brightness), analogously to the definition of the gamma in LAB space. They also have specifications in (x, y) chromaticity coordinates of the primaries red, green, and blue, and the white point (as there is no unique definition of white). The most common nonlinear RGB space is sRGB, defined by Hewlett-Packard and Microsoft in the late 1990s for use by consumer digital devices and now the default space for images on the web. The sRGB gamut is the convex hull of the red, green, and blue points, and is shown on the chromaticity diagram in figure 4.

7 Digital Image Manipulation

Digital images are typically stored as 8-bit RGB images, that is, as arrays $A \in \mathbb{R}^{m \times n \times 3}$ where a_{ij1} , a_{ij2} , and a_{ij3} are the RGB values of the pixel indexed by (i, j) . In practice, each element a_{ijk} is an integer in the range 0 to 255, but for notational simplicity we will assume the range is instead $[0, 1]$. Image manipulations correspond to transforming the array A to another array B , where

$$b_{ijk} = f_{ijk}(a_{ijk}),$$

for some functions f_{ijk} . In practice, the $3mn$ functions f_{ijk} will be highly correlated. The simplest case is where $f_{ijk} \equiv f$ is independent of i , j , and k , and an

example is $f_{ijk}(a_{ijk}) = \min(a_{ijk} + 0.2, 1)$, which brightens an image by increasing the RGB values of every pixel by 0.2. Another example is

$$f_{ijk}(a_{ijk}) = \begin{cases} 2a_{ijk}^2 & a_{ijk} \leq 0.5, \\ 1 - 2(1 - a_{ijk})^2 & a_{ijk} \geq 0.5. \end{cases} \quad (3)$$

This transformation increases contrast because it makes RGB components less than 0.5 smaller (darkening the pixel) and those greater than 0.5 larger (lightening the pixel). These kinds of global manipulations are offered by all programs for editing digital images, but the results they produce are usually crude and unprofessional. For realistic, high quality results, the transformations need to be local and, from the photographic point of view, *proportional*. For example, the brightening transformation above will change any RGB triplet (r, g, b) with $\min(r, g, b) \geq 0.8$ to $(1, 1, 1)$, which is pure white, almost certainly producing an artificial result. The transformation (3) that increases contrast will change the colors, since it modifies the RGB values at each pixel independently.

Advanced digital image manipulation avoids these problems by various techniques, a very powerful one being to apply a global transformation through a mask that selectively reduces the effect of the transformation in certain parts of the image. The power of this technique lies in the fact that the image itself can be used to construct the mask.

However, there are situations where elementary calculations on images are useful. A security camera might detect movement by computing the variance of several images taken a short time apart. A less trivial example is where one wishes to photograph a busy scene such as an iconic building without the many people and vehicles that are moving through the scene at any one time. Here, a solution is to put the camera on a tripod and take a few tens of images, each a few seconds apart, and then take the median of the images (each pixel gets the median R, G, and B values of all the pixels in that location in the image). With luck, and assuming the lighting conditions remained constant through the procedure, the median pixel will in every case be the unobscured one that was wanted!

8 Further Reading

- [1] David Austin. What is ... JPEG? *Notices Amer. Math. Soc.*, 55(2):226–229, 2008.
- [2] David M. Hunt, Kanwaijit S. Dulai, James K. Bowmaker, and John D. Mollon. [The chemistry of John Dalton's color blindness](#). *Science*, 267:984–988, 1995.
- [3] Simon Ings. *The Eye. A Natural History*. Bloomsbury, London, 2007. ix+323 pp. ISBN 978-0-7475-9286-0.
- [4] Charles S. Johnson. *Science for the Curious Photographer: An Introduction to the Science of Photography*. A K Peters, Natick, MA, USA, 2010. x+185 pp. ISBN 978-1-56881-581-7.
- [5] Dan Margulis. *Photoshop LAB Color: The Canyon Conundrum and Other Adventures in the Most Powerful Colorspace*. Peachpit Press, Berkeley, CA, USA, 2006. xviii+366 pp. ISBN 0-321-35678-0.
- [6] Kenneth Moreland. [Diverging color maps for scientific visualization](#). In *Advances in Visual Computing*, George Bebis et al., editors, volume 5876 of *Lecture Notes in Computer Science*, Springer-Verlag, Berlin, 2009, pages 92–103.
- [7] Erik Reinhard, Erum Arif Khan, Ahmet Oğuz Akyüz, and Garrett M. Johnson. *Color Imaging: Fundamentals and Applications*. A K Peters, Natick, MA, USA, 2008. xv+1058 pp. ISBN 978-1-56881-344-8.
- [8] Gaurav Sharma and H. Joel Trussell. [Digital color imaging](#). *IEEE Trans. Image Processing*, 6(7):901–932, 1997.